

ANTI-GLITCH: TRANSIENT OR PERMANENT, A BAYESIAN VIEW

YI-MING HU, MATTHEW PITKIN, IK SIONG HENG, MARTIN A. HENDRY
SUPA, School of Physics and Astronomy, University of Glasgow
Draft version November 12, 2013

ABSTRACT

Recently, Archibald et al. (2013) reported observing a sudden spin-down or *anti-glitch* in the rotation of magnetar 1E 2259+586. Such events are rare; however this particular anti-glitch was followed by another event which Archibald et al. (2013) suggested could either be a conventional glitch or another anti-glitch. In this paper we apply Bayesian Model Selection to quantitatively determine which of these two latter events better explains the observed data. We show that two successive anti-glitch events is the favoured explanation (with a Bayes Factor of ~ 45) when compared to model consisting of an anti-glitch followed by a glitch. Further, we show that the second anti-glitch has an associated frequency change, $\Delta\nu$ of -8.15×10^{-8} Hz. We discuss the implications of these results on possible physical mechanisms behind this anti-glitch.

Subject headings:

1. INTRODUCTION

Recently, Archibald et al. (2013) discovered an unexpected anti-glitch phenomenon in magnetar 1E 2259+586. Unlike a normal glitch, which undergoes a sudden spin up, this magnetar experienced a sudden spin-down. The mechanism which caused this phenomenon is still under discussion (e.g. Tong 2013; Lyutikov 2013; Katz 2013; Huang & Geng 2013; Ouyed et al. 2013), but to our knowledge no model exactly predicted an anti-glitch prior to this discovery.

The data analysis performed by Archibald et al. (2013) shows that during the observation, 1E 2259+586 undergoes two timing events separated by 50–90 days. The first event is a certain anti-glitch, while the nature of the second event is less certain. If the second event is also an anti-glitch, it suggests that anti-glitches could have a permanent effect on the magnetar, and the magnetar should be stable after an anti-glitch occurs without requiring a normal glitch to return to a steady state. On the other hand, if the second event turns out to be a normal glitch, it suggests that the anti-glitch is not stable and a normal glitch might be necessary for the magnetar to recover to a more stable state. However, the analysis performed in Archibald et al. (2013) was unable to distinguish between these two types of glitch for the second event, based on the reduced χ^2 obtained.

Since we know very little about the mechanism behind such a rare phenomenon, any information about it could be helpful to understand its physical cause. In this paper we seek to use the data themselves to distinguish between these two models, employing the methods of Bayesian Model Selection. More specifically, we compute the ratio of the *evidence* for each model (as defined in Section 3) and investigate whether this favours one model over the other. Due to its definition, the value of the evidence is strongly dependent on the prior range adopted for any model parameters. Thus the priors for these parameters should be set carefully and objectively, and the robustness of the evidence ratio to the choice of prior should be checked.

The structure of this paper is as follows. In Section 2 we briefly review relevant details of the model for the time of arrival of pulses from the progenitor. Section 3 then describes our Bayesian inference method for carrying out model selection. Section 4 presents the results of our analysis, including our check on their robustness. Finally Section 5 summarises our conclusions.

2. TIMING MODEL

The magnetar 1E 2259+586 was routinely observed by the X-ray Telescope (XRT) onboard Swift every 2–3 weeks, with more frequent observations being made shortly after discovering the first anti-glitch event reported in Archibald et al. (2013).

The observations give information on Time Of Arrival (TOA) for X-ray pulses, which can be interpreted as the pulse phase from the magnetar. According to the lighthouse model (Lorimer & Kramer 2005), it can be further understood as the rotation phase of the pulsar.

A Pulsar's TOAs can be determined to very high precision and are usually taken as an accurate 'clock'. This property of accurate timing allows research into neutron star astrophysics, tests of general relativity and even searches for gravitational waves (Stairs 2003). In order to obtain accurate TOAs, effects that could influence TOAs should be carefully removed by dedicated software like TEMPO2 (Hobbs et al. 2006). For convenience of comparison, each TOA is translated into the Solar System Barycenter (SSB).

Together with each TOA, the X-ray flux is also recorded. An energy excess helps to pinpoint the epoch of the first glitch event, while for the second event, no obvious flux change was detected – thus contributing to the confusion of the second event's type.

Physically, the magnetar is steadily rotating, with a secular decrease believed to be due to magnetic dipole emission. The frequency ν is a function of time t , i.e. $\nu = \nu(t)$, which generally can be written as $\nu(t) = \nu_0 + \dot{\nu}t + \mathcal{O}(\dot{\nu}t^2)$.

The evolution of phase ϕ for a certain pulsar, when no (anti-)glitch happens, is just the integration of frequency,

$$\phi(t) = \int_{t_0}^t \nu(t') dt' \quad (1)$$

The phase is conventionally recorded as a cycle number, so the exact moment for the i^{th} observation of TOA t_i should represent a phase $\phi(t_i)$ close to an integer N_i , and the residual difference $\Delta\phi(t_i)$ between the theoretical prediction $\phi(t_i)$ and the actual observation N_i , is

$$\Delta\phi(t_i) = \nu_0(t_i - t_0) + \frac{1}{2}\dot{\nu}(t_i - t_0)^2 - N_i \quad (2)$$

Suppose a glitch occurred at time T_g . this will cause a sudden change in frequency and the frequency evolution after the glitch can be modelled, for $t > T_g$, as

$$\nu'(t) = (\nu_g + \Delta\nu) + (\dot{\nu} + \Delta\dot{\nu})(t - T_g)$$

where ν_g is defined as frequency before the glitch. Similarly the phase evolution can be written as

$$\phi(t) = \int_{t_0}^{T_g} \nu(t')dt' + \int_{T_g}^t \nu'(t')dt' + \Delta\phi_g \quad (3)$$

where $\Delta\phi_g$ is effectively the sudden phase change during the glitch, and $\Delta\nu$ and $\Delta\dot{\nu}$ are respectively the difference in frequency and its first derivative before and after the glitch.

Subtracting equation 1 from equation 3 then yields the difference in phase evolution between a model with an (anti-)glitch at time T_g and one in which no (anti-)glitch occurs; to second order this is given by

$$\Delta\Phi_g(t) = \Delta\phi_g + \Delta\nu(t - T_g) + \frac{1}{2}\Delta\dot{\nu}(t - T_g)^2 \quad (4)$$

We further define

$$R_i = \frac{\phi_i - N_i}{\nu}$$

as the time residual after subtracting the model predictions from the data. Here ϕ_i is the predicted pulse phase at time t_i (i.e. $\phi(t_i)$) and N_i is the exact phase at the TOA, which by definition is an integer. ν is the frequency according to the model. Together with the observed timing uncertainty σ_i , we can form

$$\chi^2 = \sum_{i=1}^N \left(\frac{R_i}{\sigma_i} \right)^2 \quad (5)$$

In the next Section we will define the likelihood as proportional to $\exp(-\chi^2/2)$, and use it to evaluate the evidence for each model.

3. BAYESIAN INFERENCE

In Bayesian Inference, given prior information \mathcal{I} , and observed data D , the posterior probability $p(\theta|D, \mathcal{I})$, for a certain theoretical parameter set θ describing a model \mathcal{M} , can be expressed using Bayes' theorem as

$$p(\theta|D, \mathcal{M}, \mathcal{I}) = \frac{p(D|\theta, \mathcal{M}, \mathcal{I})p(\theta|\mathcal{M}, \mathcal{I})}{p(D|\mathcal{M}, \mathcal{I})} \quad (6)$$

Here $p(D|\theta, \mathcal{M}, \mathcal{I})$ is the *likelihood*, i.e. the probability of obtaining the observed data D given prior information \mathcal{I} , a particular set of parameters θ for model \mathcal{M} and prior information \mathcal{I} . $p(\theta|\mathcal{M}, \mathcal{I})$ is the *prior* probability for the parameters θ of model \mathcal{M} and $p(D|\mathcal{M}, \mathcal{I})$ is the *evidence*, i.e. the probability the obtaining the observed data given that model \mathcal{M} is true.

Practically the evidence is defined as

$$p(D|\mathcal{M}, \mathcal{I}) = \int_{\Theta} p(\theta|\mathcal{M}, \mathcal{I})p(D|\mathcal{M}, \theta, \mathcal{I})d\theta \quad (7)$$

In other words the evidence is calculated by marginalising the likelihood over the space of the model parameters. It is then obvious that the calculated evidence depends on the actual choice of prior range of the parameters θ .

Suppose there are several competing models \mathcal{M}_i that can explain the data. The probability for each model given the observed data D is $p(\mathcal{M}_i|D, \mathcal{I})$. Applying Bayes' theorem, we can get

$$p(\mathcal{M}_i|D, \mathcal{I}) = \frac{p(D|\mathcal{M}_i, \mathcal{I})p(\mathcal{M}_i|\mathcal{I})}{p(D|\mathcal{I})}. \quad (8)$$

The *odds ratio* for two different models \mathcal{M}_i and \mathcal{M}_j can be constructed as

$$O_{ij} = \frac{p(\mathcal{M}_i|D, \mathcal{I})}{p(\mathcal{M}_j|D, \mathcal{I})} = \frac{p(D|\mathcal{M}_i, \mathcal{I})p(\mathcal{M}_i|\mathcal{I})}{p(D|\mathcal{M}_j, \mathcal{I})p(\mathcal{M}_j|\mathcal{I})} \quad (9)$$

Normally, in the absence of further information, the prior probabilities for the two models are taken to be equal. Hence the odds ratio reduces to the ratio of the marginalised likelihoods, which known as the *Bayes Factor*. Usually, a Bayes Factor of 10 is already strong enough to favour one model against the other, while a Bayes Factor of 100 will be decisive (Jeffreys 1961).

The calculation of evidence can be a time-consuming process, the method of Nested Sampling (Skilling 2006) however makes it practicable to calculate evidence efficiently. In this work, we follow closely the method proposed in Veitch & Vecchio (2010) to calculate the Bayes factor.

4. RESULTS

In our analysis, the two models only differ in the sign of the frequency change for the second event; otherwise they share the same parameters. In order to avoid undue influence of the prior range on the Bayes Factor, we assign identical prior ranges for all common parameters in both models.

4.1. Setting the Priors

In table 1 of Archibald et al. (2013), the parameters are set to be $\nu_0 = 0.143, 285, 110 \pm (4 \times 10^{-9})s^{-1}$, $\dot{\nu} = -9.80 \pm 0.09 \times 10^{-15}s^{-2}$. The Epoch (MJD) is the time t_0 when $\nu(t_0) = \nu_0$. Since the magnetar has been observed for a long time, and the spin before the anti-glitch is not of our interest, we fix these parameters to be constants.

In both models, there are two independent (anti-)glitch events, for each event there are 4 parameters to describe: the Epoch t , and the glitch-caused changes in the frequency $\Delta\nu$, frequency first derivative $\Delta\dot{\nu}$ and the phase $\Delta\phi_g$. So, in total there are eight parameters in each model. In order to let the two models share the same parameters, we suppose that in the second model, after the normal glitch, the frequency becomes $\nu_g = \nu - \Delta\nu$ instead of $\nu_g = \nu + \Delta\nu$. In that case, $\Delta\nu$ for the second event in both model is always non-negative. In such design, two models can have exactly the same prior, so that it has least amount of influence on the final value of the Bayes Factor.

For the epoch of the first anti-glitch event, since there is an obvious change in flux between 19th and 20th

TABLE 1

MAXIMUM AND MINIMUM BAYES FACTORS OBTAINED FOR 10 DIFFERENT NOISE REALISATIONS OF THE ANALYSIS, WITH PRIORS RANGES SPANNING 10, 5 AND 3 TIMES THE UNCERTAINTIES QUOTED IN ARCHIBALD ET AL. (2013) (SAME ABSOLUTE VALUE ON $\Delta\nu_2$).

n value	10	5	3
Maximum	54.4	47.9	53.3
Minimum	38.2	39.0	45.9

observation, the prior is set to be flat between these two observations. For other parameters, there is no such obvious boundary available, however, in Archibald et al. (2013), their estimated values θ together with uncertainties σ^θ are given by TEMPO2. In order to be conservative, a range of at least $2n$ times of the uncertainty is set, where n is a variable that can be changed. For each parameter, the lower boundary is $\min(\theta_{M1} - n\sigma_{M1}^\theta, \theta_{M2} - n\sigma_{M2}^\theta)$, while the upper boundary is set to be $\max(\theta_{M1} + n\sigma_{M1}^\theta, \theta_{M2} + n\sigma_{M2}^\theta)$. Note however that $\Delta\nu$ of the second (anti-)glitch event is always non-negative, its lower limit is set to be $\min(0, \theta_{M1}^{\Delta\nu} - n\sigma_{M2}^{\Delta\nu}, \theta_{M1}^{\Delta\nu} - n\sigma_{M2}^{\Delta\nu})$, as Mi refers to the i^{th} model.

4.2. Comparing the Models

To calculate the evidence, a nested sampling code was applied with a stopping criterion set to equal e^{-5} , i.e. when new live point contribute an addition of evidence smaller than e^{-5} of the total evidence, the nested sampling code will be stopped. The value of n used for setting prior is set to be 10, so that it is far beyond the 5σ region, this conservative choice of prior guarantees that prior has as small influence on evidence as possible. The two models have evidence of $\sim e^{-33}$ and $\sim e^{-29}$ separately, which gives a Bayes Factor of ~ 45 , supporting the successive anti-glitch model over the anti/normal glitch pair model. According to the definition of Jeffreys (1961), a Bayes Factor of 45 is already very strong evidence in favour of the successive anti-glitch model.

The posterior distribution was resampled appropriately from nested sampling results, and was drawn on each pair of parameters. In figure 1 we show the posterior of parameters related to the second anti-glitch event.

We change the n to be 5 and 3 for comparison. As shown in table 1, the Bayes Factor may fluctuate around 45 for different prior range and for different realisations of nested sampling. However, the conclusion is still robust.

The best fitting parameters shows an Epoch of second event to be MJD 56088.4, the $\Delta\nu$ to be -8.15×10^{-8} Hz, the $\Delta\dot{\nu}$ to be 5.2×10^{-15} Hz/s, and the phase change to be -0.012 .

The contour line of posterior in parameter space related to the second anti-glitch is shown in figure 1. The lines corresponds to 68.3%, 95.5% and 99.7% of the maximum posterior.

4.3. Robustness Check

The timing residuals, after deducting the best fitting model, are shown in the upper panel of figure 2. This consistency confirms that two (anti-)glitch events can explain the observed date quite well.

However, as shown in lower panel of figure 2, if only considering one event, the timing residual will quickly diverge away from zero. It will be very hard to fit the data well enough to be consistent with its error bar, showing a

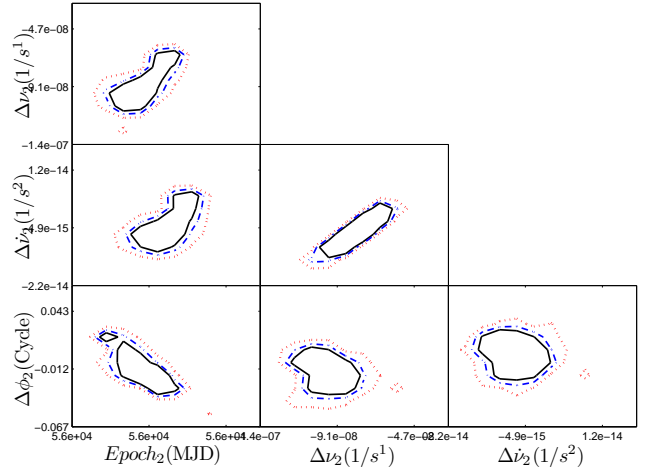


FIG. 1.— Posterior contours in parameter space for the second anti-glitch event, with 68.3% (dotted), 95.5% (dash-dotted) and 99.7% (solid) maximum posterior.

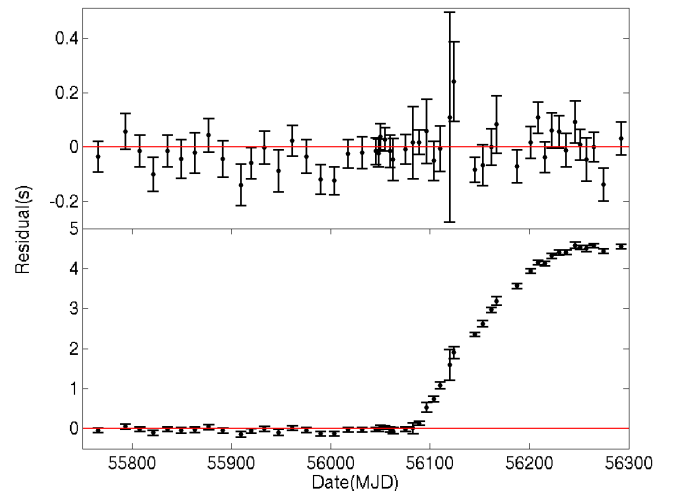


FIG. 2.— Upper panel: Timing residual of observed data for two successive anti-glitch events, with best fit parameters as determined by our analysis; Lower panel: Timing residual of observed data for only one anti-glitch event. Clearly, two anti-glitch events better explain the data than having a single anti-glitch.

strong support for the existence of a second timing event. Note that the timing residuals for an anti/normal glitch pair model are also similar to the upper panel in figure 2, further supporting the case for a second timing event.

So far, there have been some physical models proposed in order to explain the observed anti-glitch event. Among those models, some suggest that the second timing event is not consistent with the physical model, and the evidence for the second event is not strong enough. Here we also applied the similar model selection scheme to 2 timing events versus 1 anti-glitch, and the Bayes Factor turns out to be e^{208} , dominantly favouring the 2 events scenario. This results demonstrates how the Bayes Factor would favour a more complicated model, when the measurement is very accurate and a simple model can't give a satisfactory fit.

A batch of simulated data is also generated with Gaussian assumption and using fitted 1σ values from TEMPO2 for the TOA data. Nested sampling is applied on this simulated glitch-free data, and the Bayes factor of

successive anti-glitch model over anti/normal glitch pair is carried out. We calculated 15 Bayes Factor based on 15 realisations of fake data, and the Bayes Factors are fluctuating around unit ($\exp(0.17 \pm 0.33)$), showing that intrinsic randomness among data won't cause preference of one model over the other.

5. CONCLUSION AND DISCUSSION

We have shown that a model with two successive anti-glitches better explains the observed pulsar data presented in Archibald et al. (2013) when compared with an anti/normal glitch pair model. Our analysis was robust against variations in the prior ranges, with a Bayes Factor consistently around 45 in favour of two anti-glitches.

Following the discovery of this anomalous anti-glitch event, several mechanisms have been proposed seeking to explain its physical origin. Mechanisms responsible for glitches of normal pulsars, which could be caused by the coupling of the outer slow spinning crust with the inner fast rotating superfluid core (Link & Epstein 1996), cannot be reasonably used to explain the anti-glitch, since otherwise they would indicate that the core spin down even faster than the crust. Hence these models look for other causes to explain the sudden spin down. Roughly speaking, we can divide the causes into two groups: one appealing to accretion to explain the sudden decrease in angular momentum (Katz 2013; Huang & Geng 2013; Ouyed et al. 2013), while the other appealing to a structure change in the magnetosphere (Lyutikov 2013; Tong 2013).

Although the theories within each of these two groups may be quite different, the magnetosphere theories both disfavour the existence of the second timing event, while the accretion scenarios are all sufficiently flexible to explain the second event, whether it is an anti-glitch or a normal one.

In Ouyed et al. (2013), the author suggests that as an AXP, 1E 2259+586 is surrounded by a Keplerian ring and the previous burst can cause this Keplerian ring reverse its direction of angular momentum. They identify the 2002 burst to be the source, and successive anti-glitches can be explained by the reversing of multiple rings.

In Katz (2013); Huang & Geng (2013), the anti-glitch is caused by accretion of ‘‘propeller’’ surrounding materials. Previously the accretion models were challenged due to the lack of observation of an accretion disk. However, accretion of objects like planetesimals, as suggested by Huang & Geng (2013), can explain both the observed anti-glitch and the lack of evidence for an accretion disk.

Tong (2013) uses an enhanced particle wind to explain the observed anti-glitch effect, and argues that this timing event is not short in time scale, while glitches are expected to happen over a very short time. This paper also makes the prediction that every such timing event must be accompanied by a radiative event. Since during the second event, the observed luminosity shows no evidence of strong fluctuation, there seems to be limited support for the particle wind explanation.

Lyutikov (2013) on the other hand explains the anti-glitch with a CME-type mechanism, i.e. a structure change in the magnetosphere. The intrinsic highly variable property of such a mechanism alone would explain the timing property of 1E 2259+586; thus a second (anti-)glitch is not necessary.

According to our analysis, a model that can produce two successive anti-glitches is clearly favoured by the data. In general, all accretion theories are able to generate a second anti-glitch event, while neither magnetospheric mechanism makes a strong prediction of the existence of a second timing event. In general, therefore, the accretion models are preferred by the timing data themselves, in the absence of any other extrinsic information about the mechanism. Note that magnetospheric mechanism could still be valid, as the idea of magnetar does not appeal to a complicated model to explain the consistent behaviour between normal pulsars and magnetars; this simplification could mean that the prior odds ratio is more favourable for a magnetospheric mechanism, thus balancing the effect of the Bayes Factor and resulting in a posterior odds ratio that favours it. Nevertheless, Lyutikov (2013) pointed out that glitch events, although having similar behaviour to a normal pulsar glitch and in a magnetar, should be intrinsically very different. Further investigation is thus needed to obtain a definitive conclusion about the physical mechanism behind anti-glitches.

6. ACKNOWLEDGMENTS

The authors would like to thank Robert Archibald, Victoria Kaspi and Neil Gehrels for helping with the data and discussions. We are also grateful for further useful discussions with Jonathan Katz, Yongfeng Huang and Hao Tong. The authors gratefully acknowledge the support of the Science and Technology Facilities Council of the United Kingdom and the Scottish Universities Physics Alliance. Y.-M. Hu was supported by the China Scholarship Council.

REFERENCES

- Archibald, R. F., Kaspi, V. M., Ng, C. Y.,ourgouliatos, K. N., Tsang, D., Scholz, P., Beardmore, A. P., Gehrels, N., & Kennea, J. A. 2013, *Nature*, 497, 591
- Hobbs, G. B., Edwards, R. T., & Manchester, R. N. 2006, *MNRAS*, 369, 655
- Huang, Y. F. & Geng, J. J. 2013, arXiv:1310.3324
- Jeffreys, H. 1961, *Theory of Probability* (3rd Edition) (New York: Oxford University Press)
- Katz, J. I. 2013, arXiv:1307.0586
- Link, B. & Epstein, R. I. 1996, *ApJ*, 457, 844
- Lorimer, D. & Kramer, M. 2005, *Cambridge Observing Handbooks for Research Astronomers*, Vol. 4, *Handbook of Pulsar Astronomy*, 1st edn. (Cambridge, U.K.; New York, U.S.A: Cambridge University Press)
- Lyutikov, M. 2013, arXiv:1306.2264
- Ouyed, R., Leahy, D., & Koning, N. 2013, arXiv:1307.1386
- Skilling, J. 2006, *Bayesian Analysis*, 1, 833
- Stairs, I. H. 2003, *Living Reviews in Relativity*, 6
- Tong, H. 2013, arXiv:1306.2445
- Veitch, J. & Vecchio, A. 2010, *Phys. Rev. D*, 81, 062003